



Predicted ultimate strength for the design of deep beams with shear openings

Prof. M. A. Ibrahim, Prof. A. El Thakeb, Prof. A.A. Mostfa, and Eng. H. Ali Kottb

Civil Engineering Department, Faculty of Engineering Al-Azhar University

ملخص البحث:

يقدم هذا البحث دراسة تحليلية تأكيدية علي التجارب العملية الخاصة بدراسة كفاءة نماذج جديدة لتسليح الكمرات العميقة ذات فتحات القص مختلفة المقاسات، اضافة الي صيغة مقترحة لتصميم هذا النوع من الكمرات. أثبتت نتائج الدراسة التحليلية كفاءة الأساليب والنماذج المقترحة من خلال التوافق بين قدرة تحمل الكمرات المختبرة ومثيلاتها التي تم تحليلها ببرنامج ABAQUS بمتوسط 97% بالنسبة لحمل الانهيار و 69% بالنسبة للترخيم عند أقصى حمل في كل مجموعات البرنامج العملي. وشمل هذا البرنامج التحليلي دراسة عدد 14 كمرة تمثل مجموعتان مختلفتان من اجهاد الخرسانة، وثلاثة مقاسات مختلفة لفتحة القص. وكشفت المقارنة عن دقة النموذج التحليلي المستخدم في تمثيل الكمرات الخرسانية العميقة المصمتة والتي بها فتحات، وشملت المقارنة: التنبؤ بحمل الكسر وسلوك تلك الكمرات وكذلك شكل الشروخ واجهاد حديد التسليح المقترح في منطقة القص حول الفتحات، في حين اتضح أن النموذج متحفظ قليلا في التنبؤ بحمل الانهيار للكمرات العميقة المصنوعة من خرسانة ذات رتبة عالية والتي بها فتحات كبيرة في منطقة القص. باستخدام كلا من برنامج ABAQUS ومواصفات الكود الأمريكي للخرسانة [1] ACI 318-14، تم استحداث دراسة موسعة للعلاقة بين مقاس الفتحات في منطقة القص من ناحية ونسبة حمل الانهيار لهذه الكمرات الي حمل الانهيار لنظيراتها المصمتة من ناحية أخرى. وأسفرت هذه الدراسة عن اقتراح صيغة محايدة لحساب حمل الانهيار للكمرات الخرسانية العميقة التي بها فتحات في منطقة القص، والتي ينصح باستخدامها عند تصميم مثل هذه الكمرات ذات نفس نسبة بحر القص الي العمق.

Abstract

This research presents an analytical study to verify the experimental study of new models for reinforcing deep beams with different shear openings, in addition to proposing a formula for calculating the shear capacity of such beams.

The results of the analytical study demonstrated the efficiency of the proposed nonlinear finite element (NLFE) model by matching the carrying capacity of the tested beams and their comparative analyzed by the ABAQUS program with an average of 97% for the ultimate load and 69% for the deflection at maximum load in all experimental program groups. The analytical program included representing a 14-specimens study with two different concrete strength and three different sizes of shear openings.

The comparison revealed the accuracy of the analytical model in the representation of solid deep beams and deep beams with shear openings; including predicting the fracture load, the behavior of these beams, in addition to the crack pattern and Stresses of the proposed reinforcement configurations. While the model is slightly conservative in predicting the ultimate load of deep beams with large openings and higher compressive strength.

Using both of ABAQUS program and specifications of the ACI 318-14 [1], a parametric study was developed to investigate the relationship between shear strength of deep beams with different sizes of shear openings and shear opening ratio to the total area of shear zone.

Based on this parametric study, a dimensionless formula for calculating the shear strength of deep beams was obtained, which can be utilized in the design of such beams which have the same shear span-to-depth ratio.

Keywords: *Solid deep beams, deep beams with shear openings, proposed reinforcement, finite element modeling.*

1. Introduction

The finite element analysis (FEA) has wide applicability for both science and engineering issues. In structural engineering field, it can deal with models of various boundary conditions, unusual geometry, and different loading cases/types (including static and dynamic loads)

Nonlinear strain distribution along deep beam depth must be taken in consideration to understand the behavior of deep beams with opening. Using FEA in studying the effect of web openings on the load capacity and behavior of reinforced concrete deep beams overcome that issue.

The ACI 318-14 [1] and ECP 203-2007 [2] define the deep beam with two conditions as follow: beam with shear span-to-depth ratio less than or equal to 2 or beam with clear span less than or equal to four times its height.

ACI 318-14 [1] illustrated the method of strut-and-tie for designing and detailing of solid deep beams which based on balancing between forces in a chosen truss model unlike original beam theory in the shallow beams.

Strut-and-tie method has difficulties in choosing the optimum truss model for complicated structures and predicting the mode of failure.

Previous researches concentrated upon studying the effect of opening existence on the load capacity of the deep beam such as;

G. Campione and G. Minafo (2012) [3] tested twenty deep beams with and without openings in flexure under four-point loading to investigate the effect of Circular openings. They found that the effect of hole in deep beams depends on its position, they also suggested equation to determine the transverse tension of reinforced/unreinforced concrete struts.

A. R. Mohamed et al. (2014) [4] verified a finite element (FE) model using concrete damaged plasticity in ABAQUS program with previous experimental results, then parametric study was presented to obtain the optimum reinforcement distribution and recommendation for the maximum depth of the opening relative to the deep beam depth. El-Demerdash W. E. et al (2015) [5] made verifications on previous experimental results by FEA using ANSYS program.

This research present a FE modeling of deep beams with shear openings reinforced with new applicable reinforcement methods in addition to conclude applicable formula for predicting shear strength of deep beams with shear openings.

2. ABAQUS Concrete Damaged Plasticity (CDP) model and material properties

In this study concrete damaged plasticity (CDP) model will be used to represent concrete behavior in finite element analysis.

The CDP model has the ability to simulate the inelastic behavior of concrete in both compression and tension using damaged parameters. Modifications must be performed for the two stress-strain curves in both of tension and compression to get the optimum representation of concrete behavior as follow:

2.1. Tension stiffening relationship for concrete

In the reinforced concrete the post-failure stress-strain relation can be obtained by drawing the relation between post-failure stresses σ_{to} and cracking strain, ε_t^{ck}

The cracking strain is defined as the total strain minus the elastic strain corresponding to the undamaged material; that is, $\tilde{\varepsilon}_t^{ck} = \varepsilon_t - \varepsilon_{0t}^{el}$, where $\varepsilon_{0t}^{el} = \sigma_t/E_0$, as illustrated in figure 1

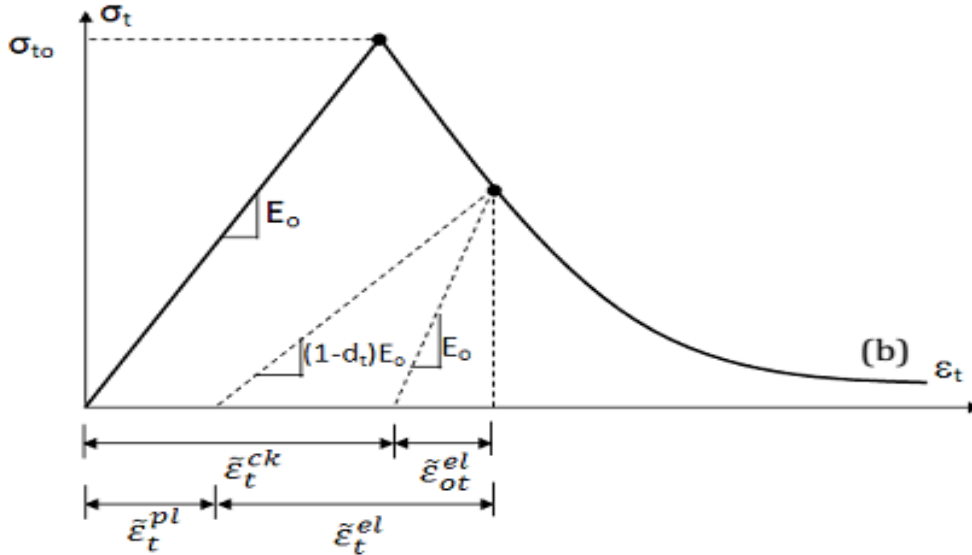


Fig. 1: Definition of tension stiffening model for concrete based on stress-strain relation, ABAQUS Analysis user's guide 2016 [6]

Nayal and Rasheed 2006 [7] approach was chosen to model the tensile stress-strain curve in ABAQUS for two concrete strengths 41 and 53 MPa

2.2. Compression behavior for concrete

Compression hardening data are given in terms of an inelastic strain, $\tilde{\varepsilon}_c^{in}$ instead of plastic strain, $\tilde{\varepsilon}_c^{pl}$. The compressive inelastic strain is defined as the total strain minus the elastic strain related to the undamaged material, $\tilde{\varepsilon}_c^{in} = \varepsilon_c - \varepsilon_{0c}^{el}$, where $\varepsilon_{0c}^{el} = \sigma_c/E_0$, as illustrated in figure 2.

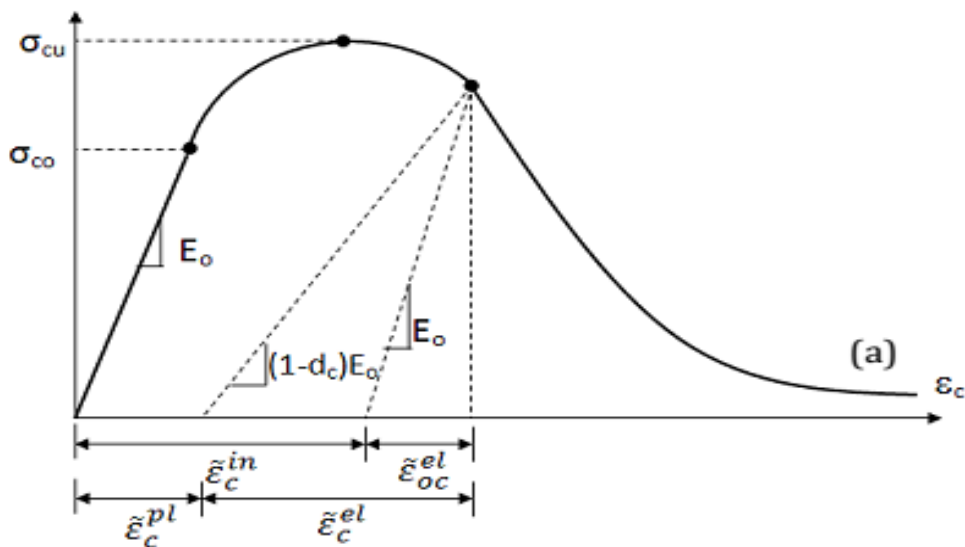


Fig. 2: Definition of concrete compression behavior in ABAQUS analysis user's guide [6]

2.3. Modeling of stress-strain curve in compression for concrete

According to Hognestad 1951[8]: Compressive stress at any point can be defined using equation 1 within range of 0 to ε_0 (strain at peak stress) which equal to $\varepsilon_0 = \frac{2f'_c}{E_c}$

Stress- strain relationship at any point from ε_0 to ε_{cu} can be obtained by equation 2

$$\sigma_c = f'_c \left[2 \frac{\varepsilon_c}{\varepsilon_0} - \left(\frac{\varepsilon_c}{\varepsilon_0} \right)^2 \right] \quad (\varepsilon_c \leq \varepsilon_0) \quad (\text{eq. 1})$$

$$\sigma_c = f'_c \left[1 - 0.15 \frac{\varepsilon_c - \varepsilon_0}{\varepsilon_{cu} - \varepsilon_0} \right] \quad (\varepsilon_0 < \varepsilon_c \leq \varepsilon_{cu}) \quad (\text{eq. 2})$$

Where $\varepsilon_{cu} = 0.004$

2.4. Material properties for reinforcing steel in the FE model

Stress-strain relationship is bilinear isotropic elastic–perfectly plastic for rebar and identical in tension and compression. The modulus of elasticity governs the relation between stress and strain till yielding point, then steel begin to deform plastically once the steel strain reach yield limit.

3. Finite element modeling of reinforced concrete deep beams

Three-dimensional nonlinear finite element analysis was performed to verify the output of FE model with the experimental results.

ABAQUS program provide both of geometric and material nonlinearity in modeling of reinforced concrete structures. ABAQUS program has ability to simulate the concrete and reinforcing steel elements with its nonlinear behavior.

Three-dimensional, eight node, solid element C3D8; was used to simulate concrete, it can represent material nonlinearity of the concrete by activate damage technique.

Using damage technique, ABAQUS program captures the mode of failure in both of tension and compression.

2-node truss element T3D2 was used to simulate reinforcing steel bars, it has ability to be embedded inside the concrete.

Bonding between concrete and reinforcing steel bars was executed by embedded constraint technique in ABAQUS, which consider concrete block as host region and steel bars as embedded region, which constrained to degrees of freedom for the host element.

4. Verification of the finite element model with experimental results

All tested deep beams have the same full span length, depth, and shear span length, the only two differences between NSC and HSC specimens are width of the beam and main tie steel. Table 1 illustrates the geometry details and section dimensions of all specimens in Ph.D experimental program [9].

Table 1: Properties and details of deep beams in the experimental study [9]

Group Descriptions	Specimen name	Dimension of openings (x*h) mm	Main tensile rft.	Comp. rft.	Web rft. (except shear zone)	Reinforcement of the openings (in Shear zone)			
						Closed short ties below & above openings	Add. Horizontal web rft. below & above openings	Add. Vertical web rft. adjacent to openings	Embedded struts
Solid NSC deep beam	NSD								
Group A (NSC deep beams with large openings)	NLR	200x180	2Φ16	2Φ12	Φ6@110 mm	2Φ6	2Φ6	2Φ6	
	NLS					2Φ6	2Φ12	2Φ10	4Φ12
	NLT					15Φ8	2Φ12	2Φ10	
Solid HSC deep beam	HSD								
Group B (HSC deep beams with large openings)	HLR	200x180	3Φ16	2Φ12		2Φ6	2Φ6	2Φ6	
	HLS					2Φ6	2Φ12	2Φ10	4Φ12
	HLT					15Φ8	2Φ12	2Φ10	
Group C (HSC deep beams with Medium openings)	HMR	150x150	3Φ16	2Φ12		1Φ6	2Φ6	2Φ6	
	HMS					1Φ6	2Φ12	2Φ10	4Φ12
	HMT					15Φ8	2Φ12	2Φ10	
Group D (HSC deep beams with Small openings)	HSR	100x120	3Φ16	2Φ12	1Φ6	2Φ6	2Φ6		
	HSS				1Φ6	2Φ12	2Φ10	4Φ12	
	HST				15Φ8	2Φ12	2Φ10		

* Section dimensions are 150x600 mm for all HSC and 120x600 mm for all NSC deep beams.

*All embedded struts have ties of 6mm @ 50 mm.

Figures 3 to 7 illustrate the section dimension and reinforcement details of the tested deep beams in the experimental program.

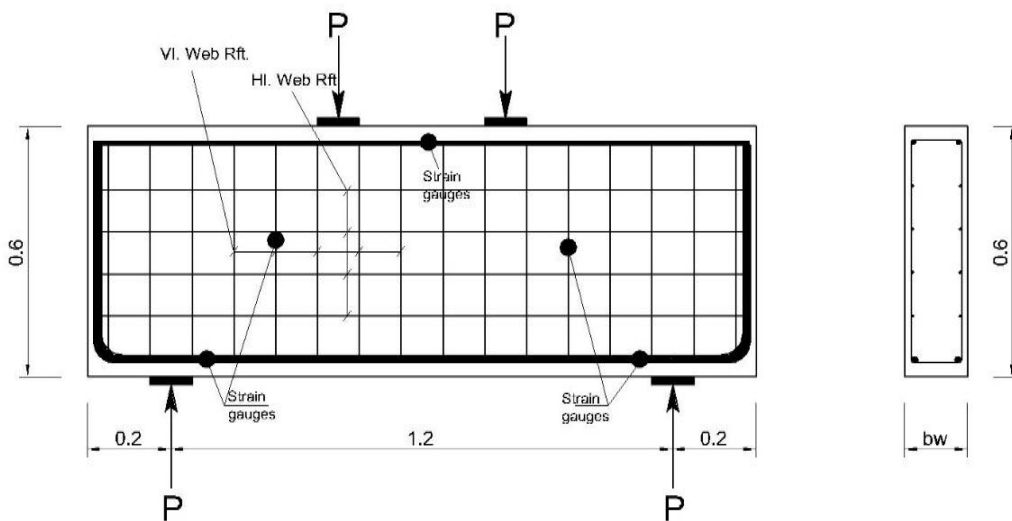


Fig. 3: Location of installed strain gauges and web reinforcement details for solid deep beams NSD and HSD.

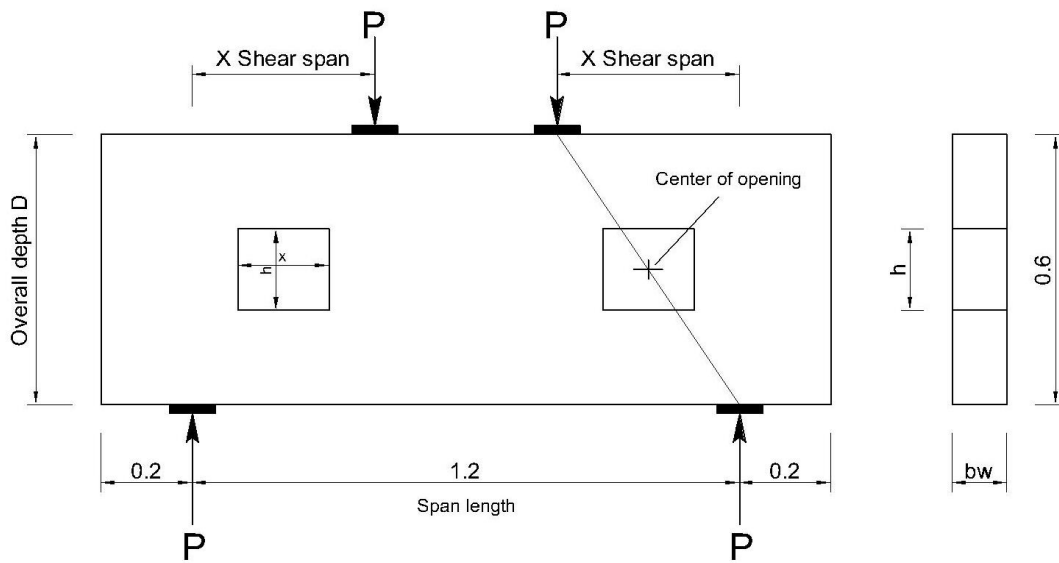


Fig. 4: General layout and section details for all deep beams with openings.

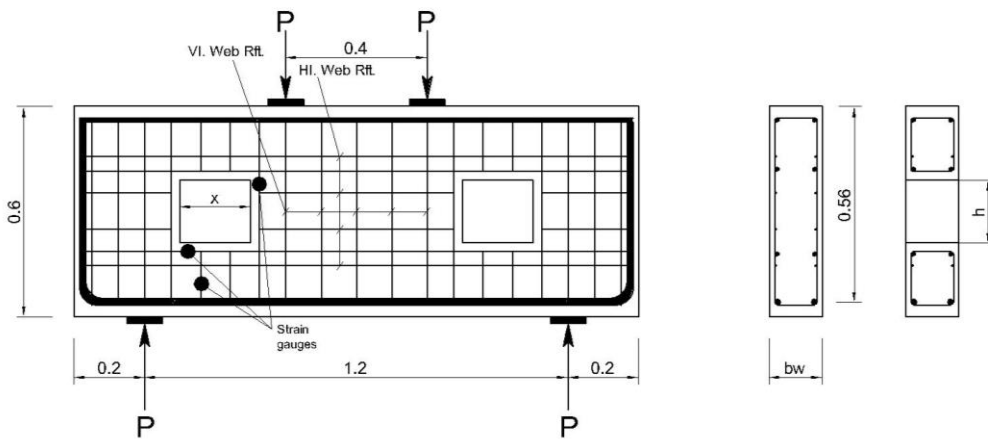


Fig. 5: Location of installed strain gauges and reinforcement details for all reference deep beams with openings.

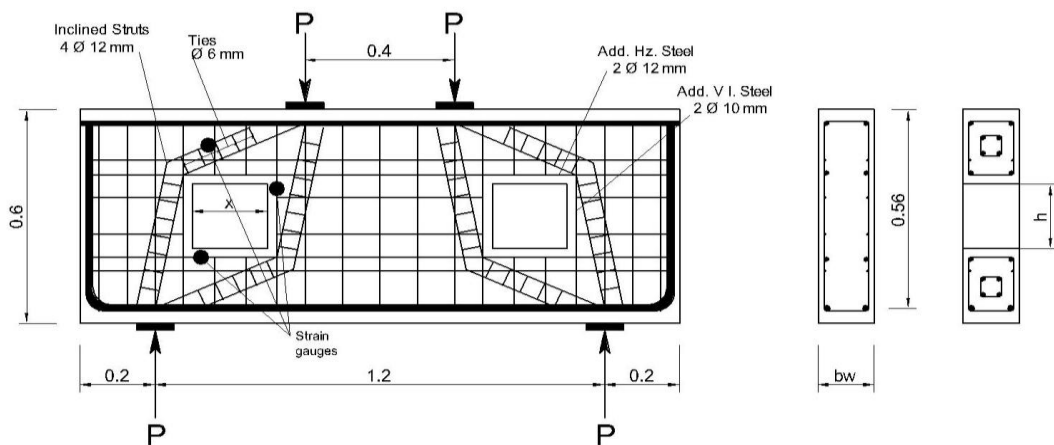


Fig. 6: Reinforcement details for all deep beams with openings reinforced with embedded struts.

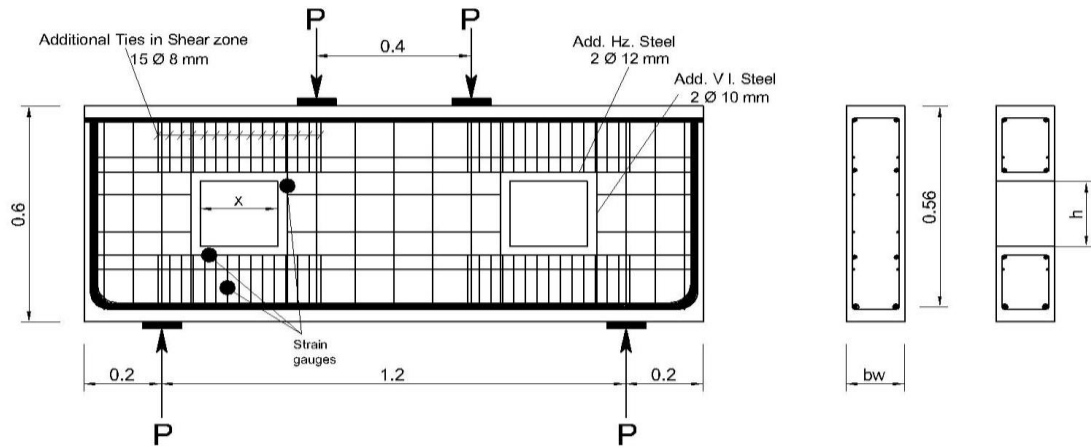


Fig. 7: Reinforcement details for all deep beams with openings reinforced with intensify ties in shear zone.

Table 2 shows comparison between results of experimental program and finite element modeling using ABAQUS program.

Table 2: Comparison between analytical and experimental results for all deep beams in the study

No.	Specimen	P_u (kN)			Deflection at ultimate load Δ (mm)		
		$P_{exp.}$	P_{ABAQUS}	$P_{ABAQUS}/P_{exp}\%$	$\Delta_{exp.}$	Δ_{ABAQUS}	$\Delta_{ABAQUS}/\Delta_{exp}\%$
1	NSD	455	443	97.36	6	2.8	46.67
2	NLR	270	259	95.93	5.02	3	59.76
3	NLS	357	327	91.60	3.64	3.37	92.58
4	NLT	381	429	112.60	5.8	4.42	76.21
5	HSD	552	560	101.45	3.58	3	83.80
6	HLR	270	252	93.33	5.13	2.6	50.68
7	HLS	369	287	77.78	4.41	3	68.03
8	HLT	407	350	86.00	8.1	3.8	46.91
9	HMR	325	300	92.31	5.1	2.5	49.02
10	HMS	400	450	112.50	3.53	3.65	103.40
11	HMT	422	519	122.99	5.9	5	84.75
12	HSR	440	400	90.91	5.09	3.4	66.80
13	HSS	623	580	93.10	5	3.2	64.00
14	HST	554	504	90.97	6.2	5	80.65
<i>Average</i>				97.06			69.52

From table 2, it can be observed that FE model is quite precise prediction of ultimate loads of deep beams without and with shear openings.

The average ratio between Abaqus and experimental ultimate loads is 97.06% which indicates the efficiency of the utilized FE model in simulating of deep beams with openings.

4.1. Comparison between cracking pattern of FE model and experimental results

Figures 8 to 21 show the crack pattern of the deep beams in the experimental program in comparing with the tensile damage of the FE model (DAMAGET,) which describe the cracks in the model due to tensile stresses.

From the following figures, they clearly show matching with each other.

In the solid deep beams and deep beams with small openings, existence of flexural cracks is obtained in the FE model.

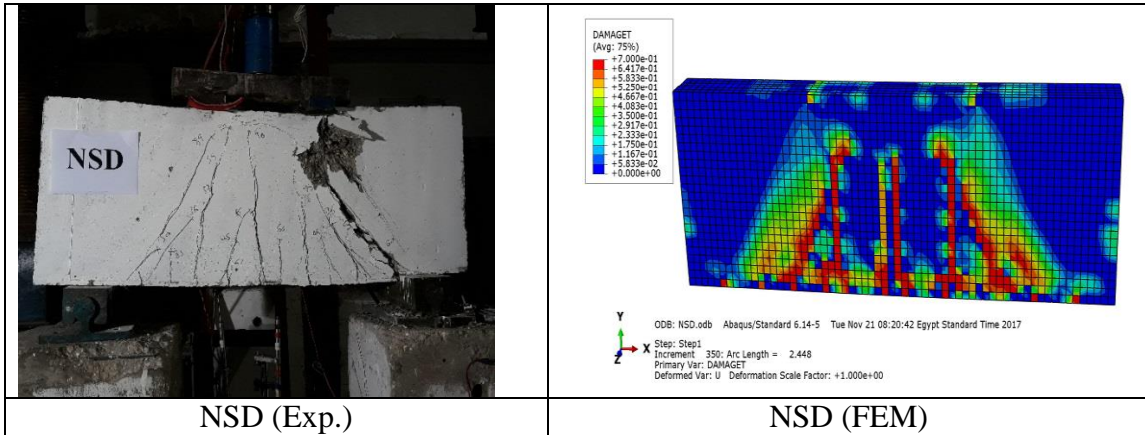


Fig.8: Crack pattern of solid deep beam NSD vs FEM tension damage

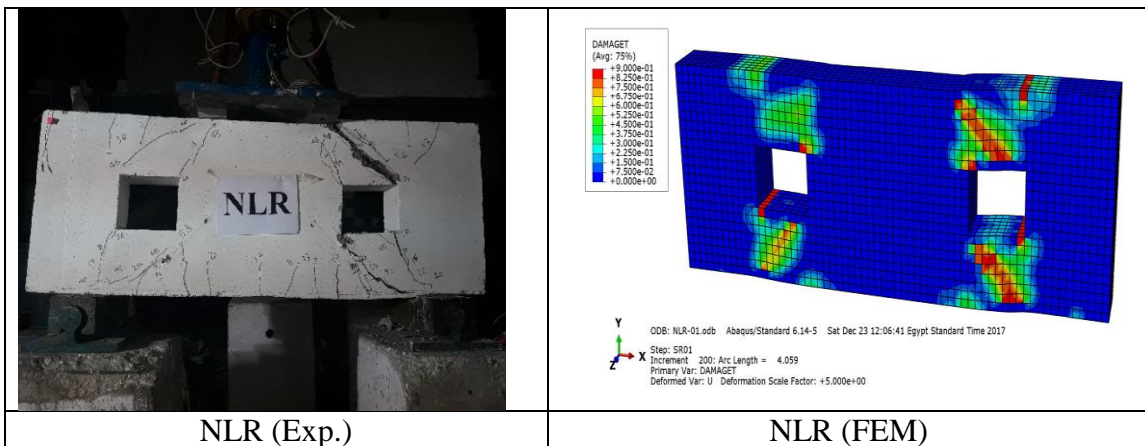


Fig.9: Crack pattern of deep beam NLR vs FEM tension damage

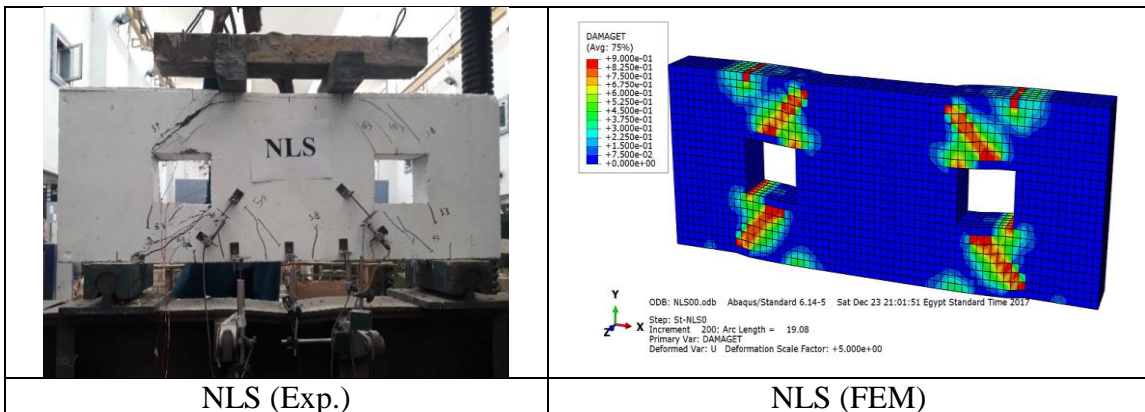


Fig.10: Crack pattern of deep beam NLS vs FEM tension damage

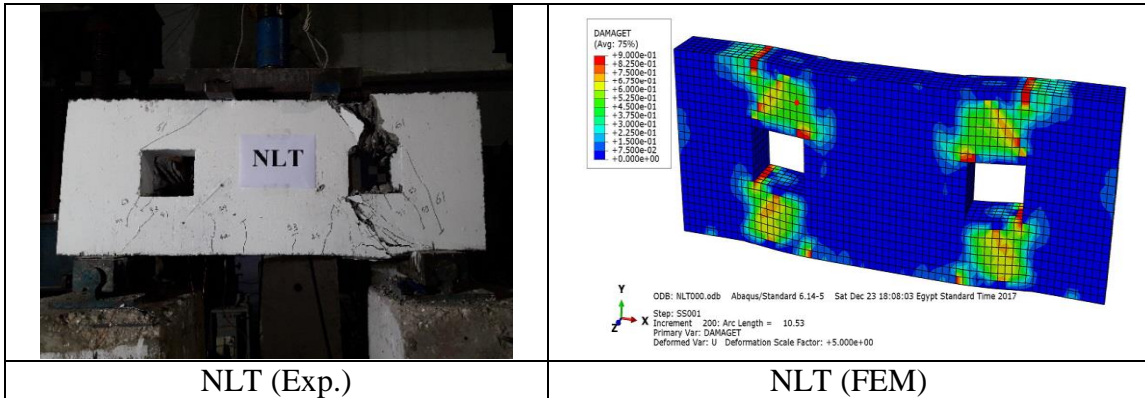


Fig.11: Crack pattern of deep beam NLT vs FEM tension damage

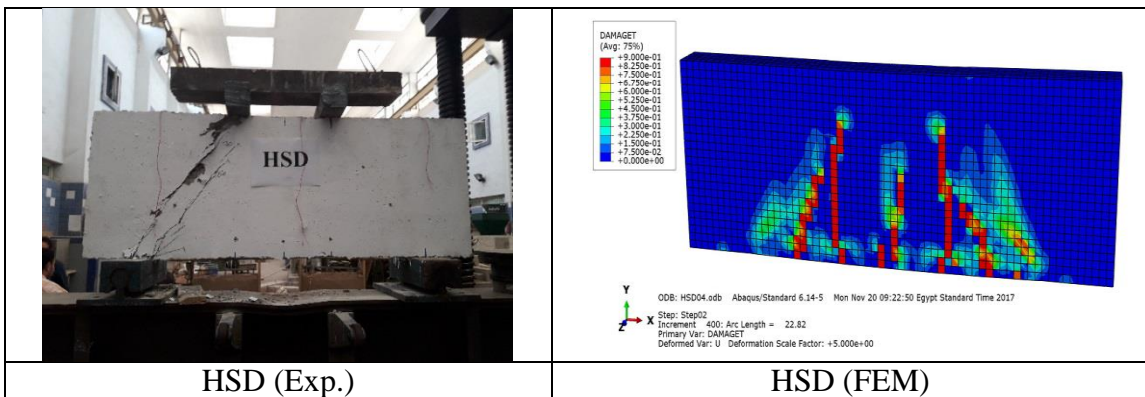


Fig.12: Crack pattern of deep beam HSD vs FEM tension damage

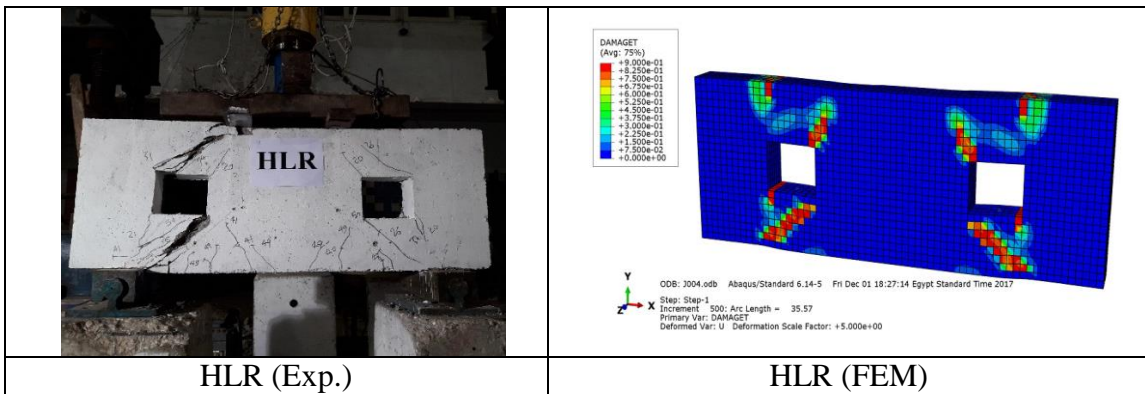


Fig.13: Crack pattern of deep beam HLR vs FEM tension damage

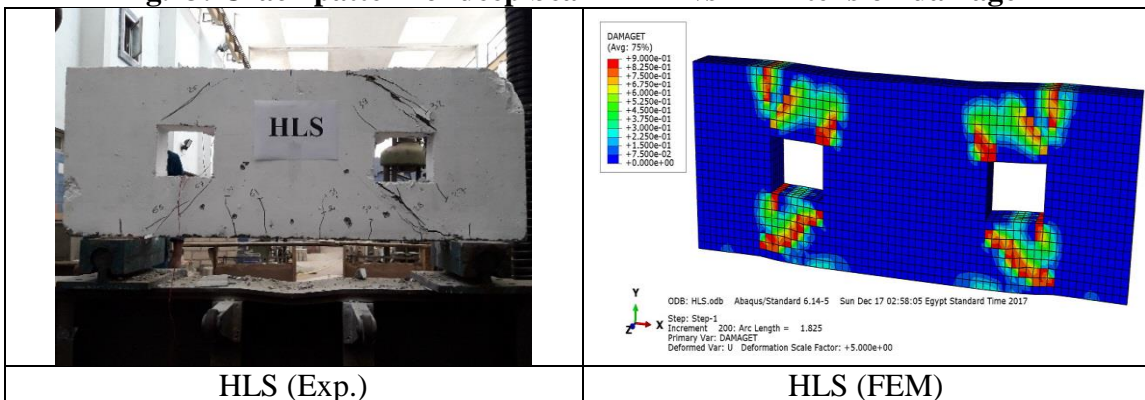


Fig.14: Crack pattern of deep beam HLS vs FEM tension damage

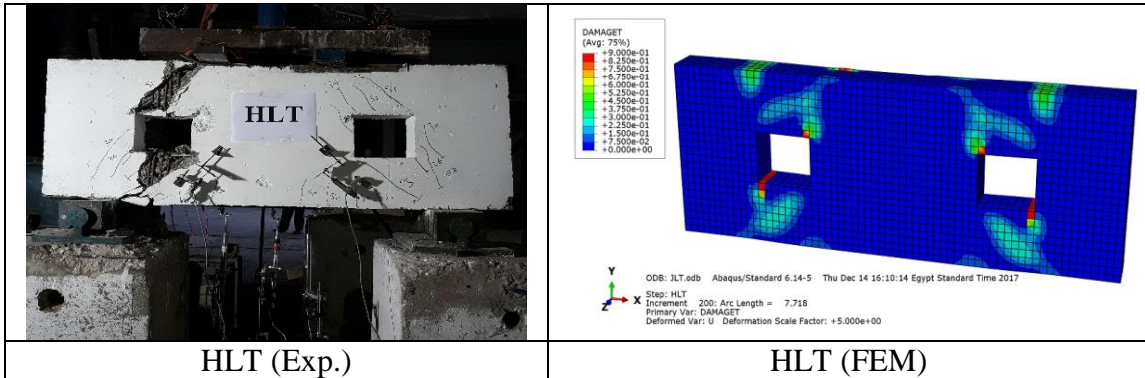


Fig.15: Crack pattern of deep beam HLT vs FEM tension damage

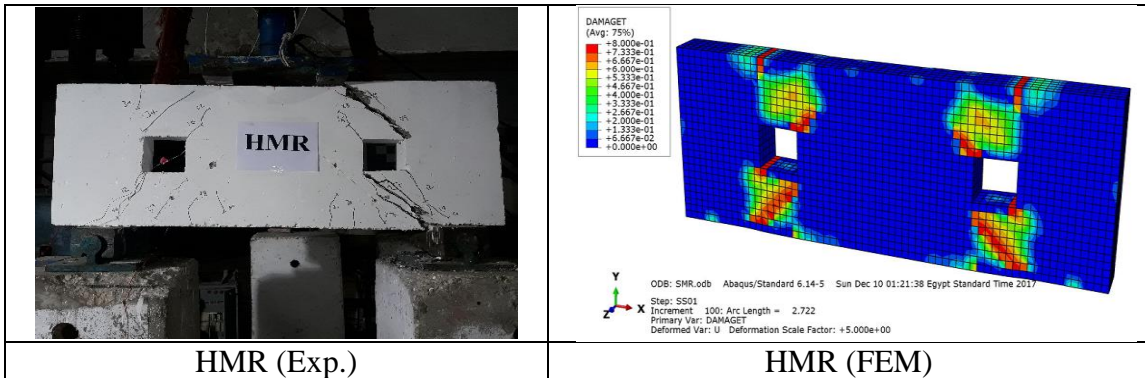


Fig.16: Crack pattern of deep beam HMR vs FEM tension damage

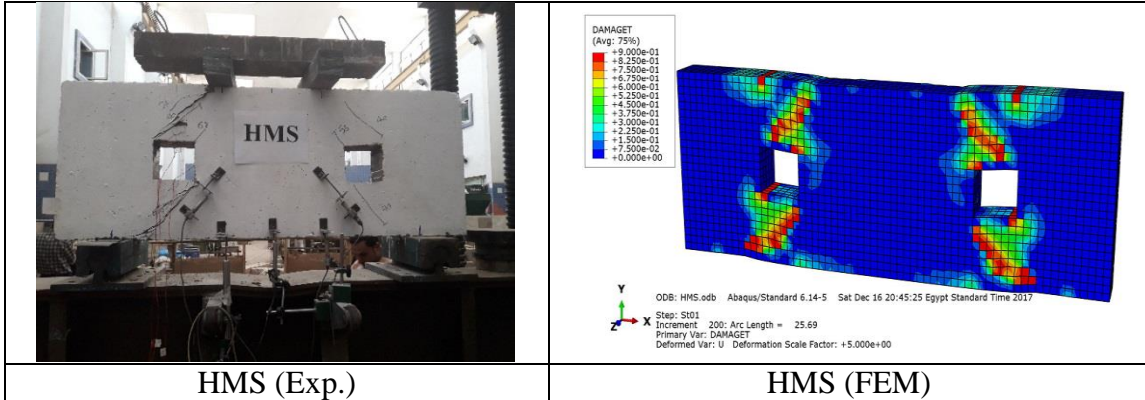


Fig.17: Crack pattern of deep beam HMS vs FEM tension damage

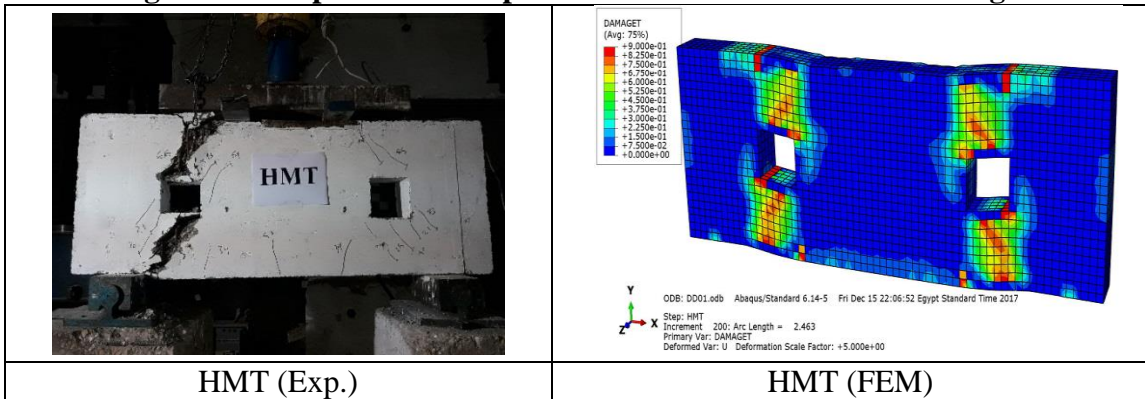


Fig.18: Crack pattern of deep beam HMT vs FEM tension damage

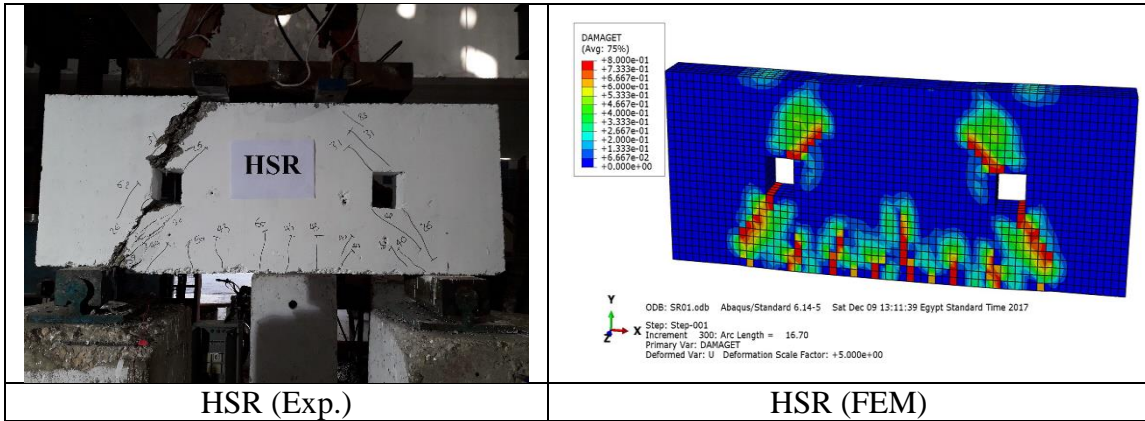


Fig.19: Crack pattern of deep beam HSR vs FEM tension damage

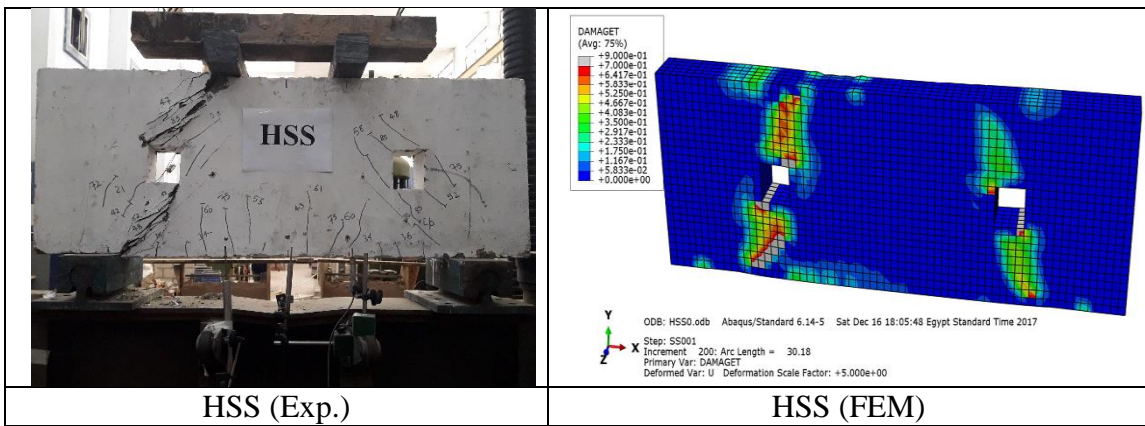


Fig.20: Crack pattern of deep beam HSS vs FEM tension damage

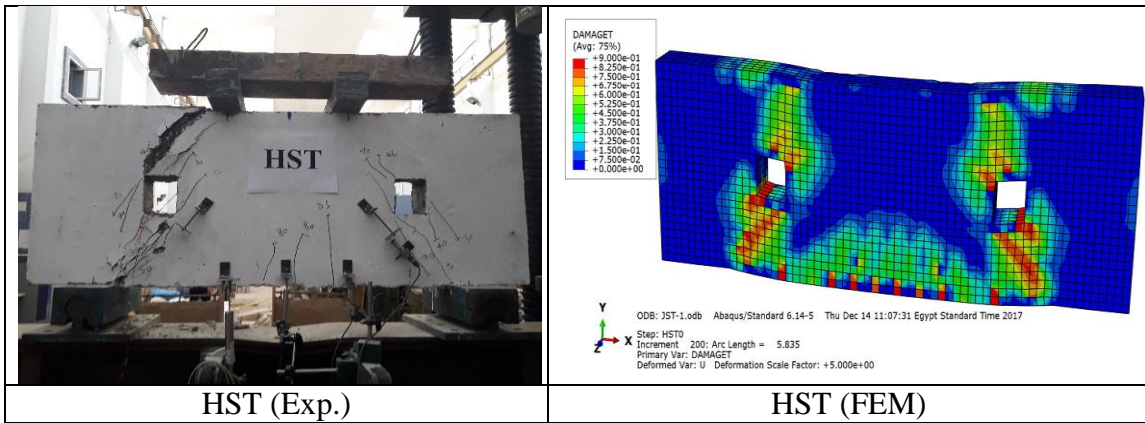


Fig.21: Crack pattern of deep beam HST vs FEM tension damage

4.2. Comparison between load-displacement responses in both experimental study and finite element model

Figures from 22 to 25 illustrate the comparison between load-mid span deflections in experimental and FE model using ABAQUS program.

From the following figures, it can be seen that FE model able to capture the real behavior of the deep beams whether in existence of shear openings or not.

Differences between the two relations were considered due to limitations on concrete to deform with damage technique in ABAQUS program.

But in general, both of FE and experimental responses have the same trend and quite closely values.

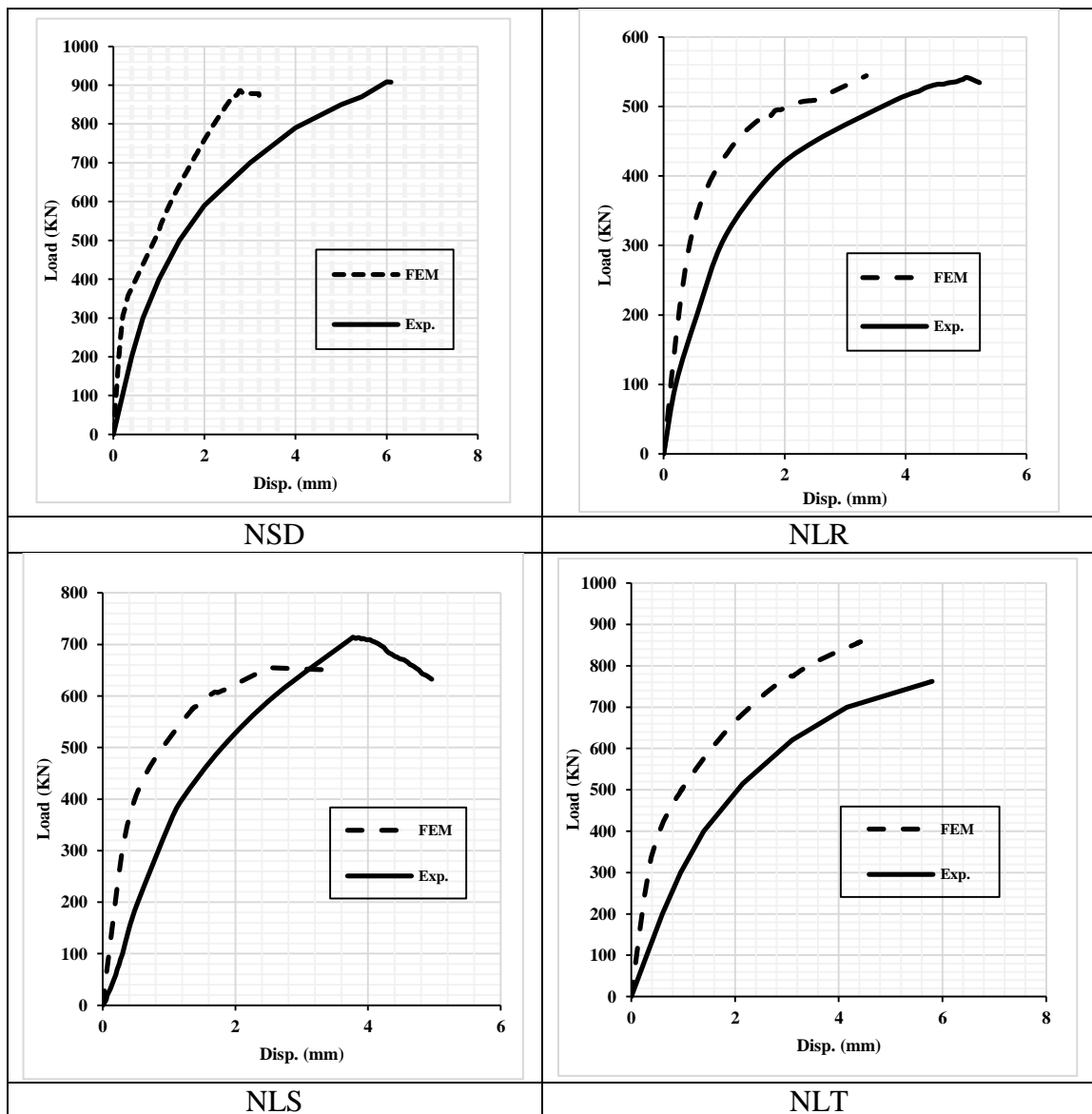


Fig. 22: Load-displacement response for beams NSD, NLR, NLS, and NLT in both experimental and FEM

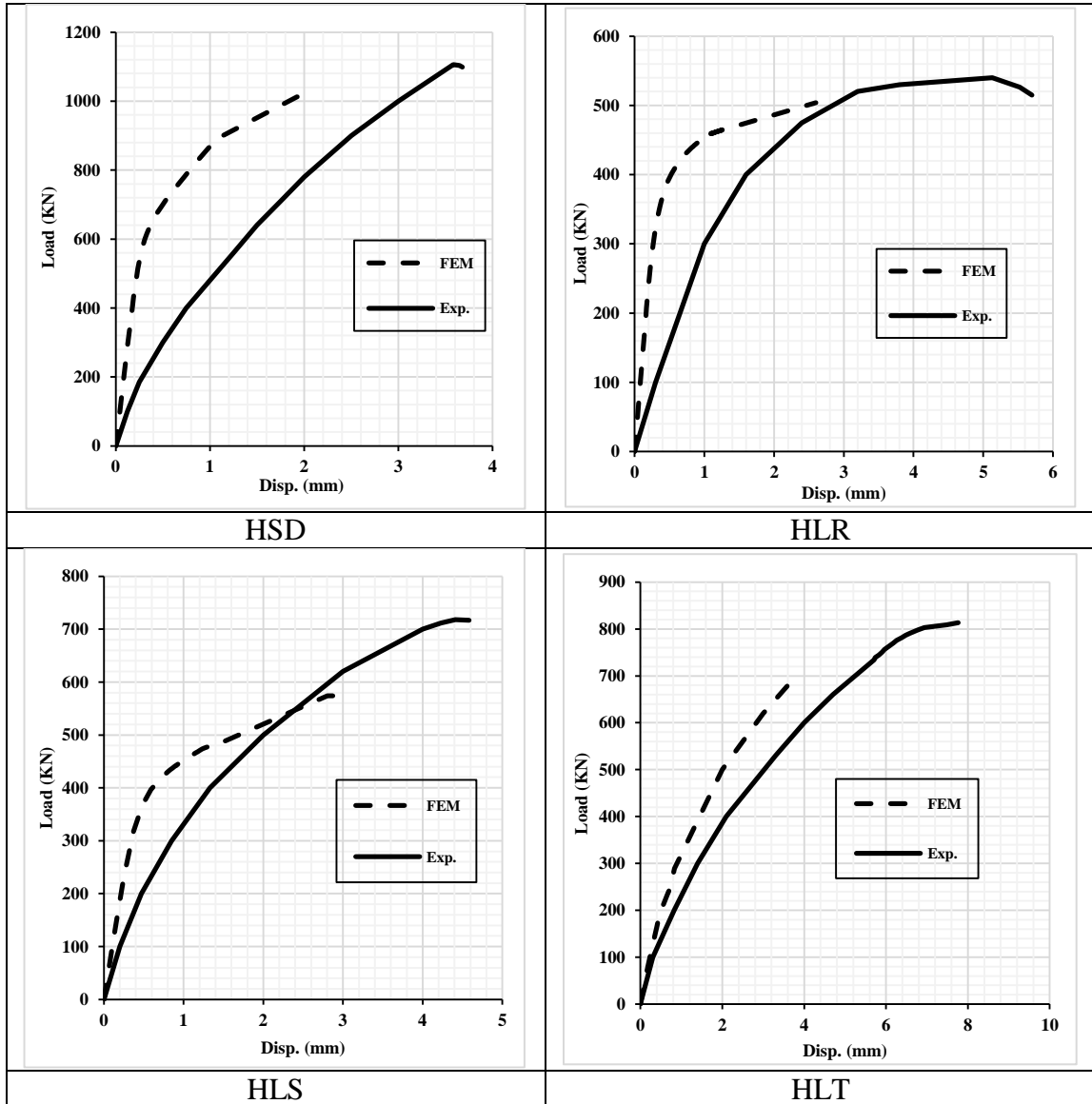


Fig. 23: Load-displacement response for beams HSD, HLR, HLS, and HLT in both experimental and FEM

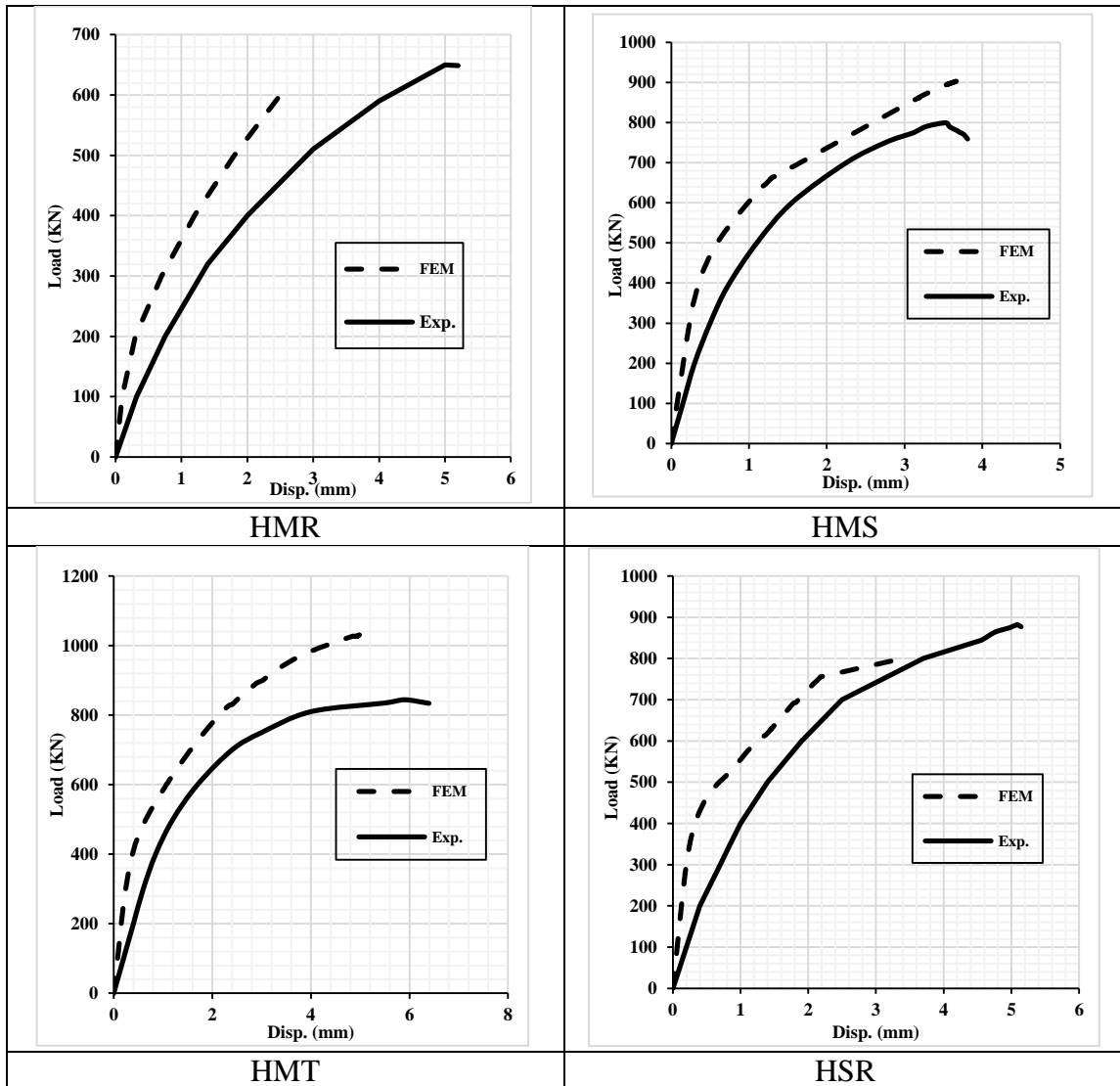


Fig. 24: Load-displacement response for beams HMR, HMS, HMT, and HSR in both experimental and FEM

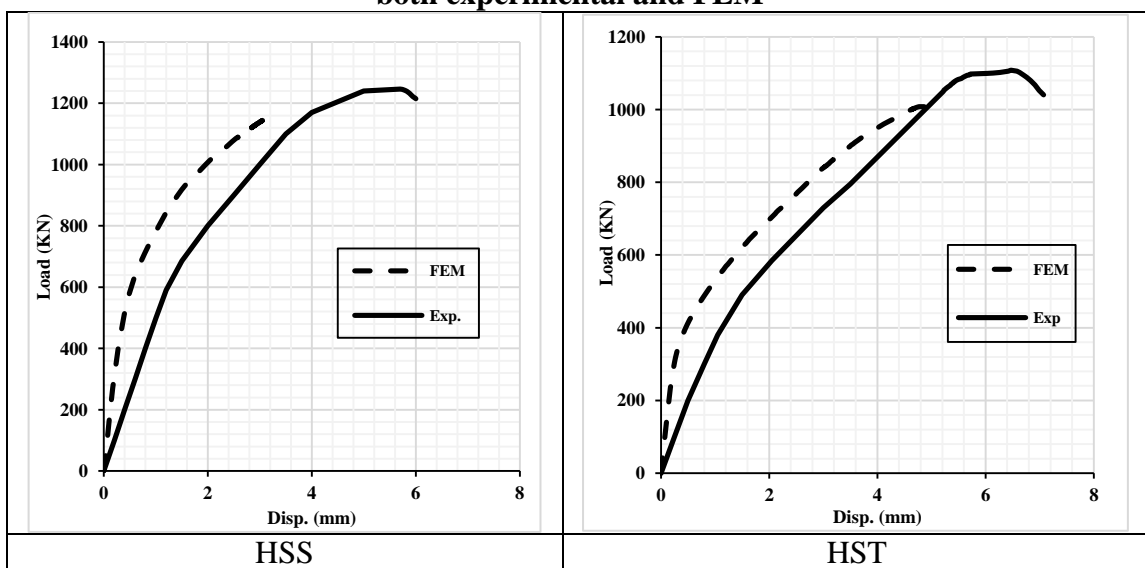
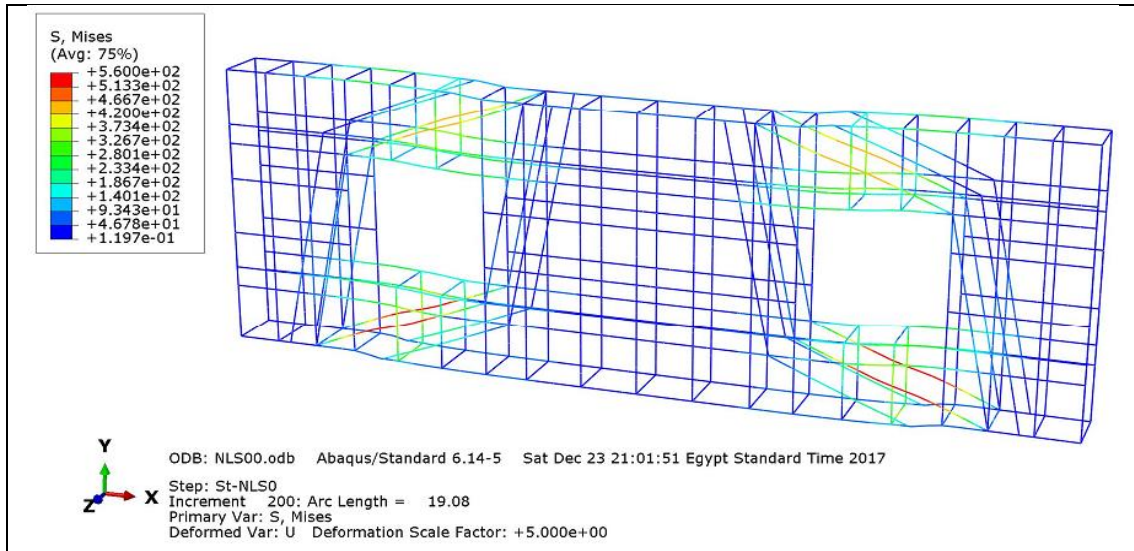


Fig. 25: Load-displacement response for beams HSS and HST in both experimental and FEM

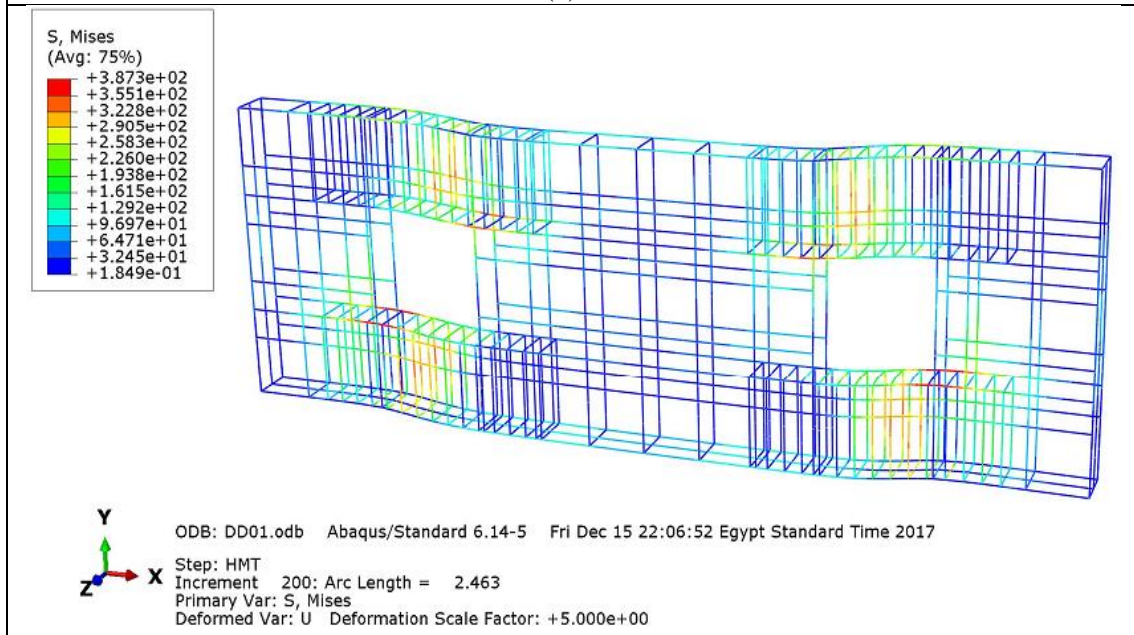
4.3. Efficiency of proposed reinforcement configurations in FEM

The efficiency of the new reinforcement configurations, of the deep beams with shear openings, can be obtained due to yielding of those reinforcement component.

Figure 26 and 27 show the stresses of the proposed reinforcement models of the deep beams with openings.



(a) NLS



(b) HMT

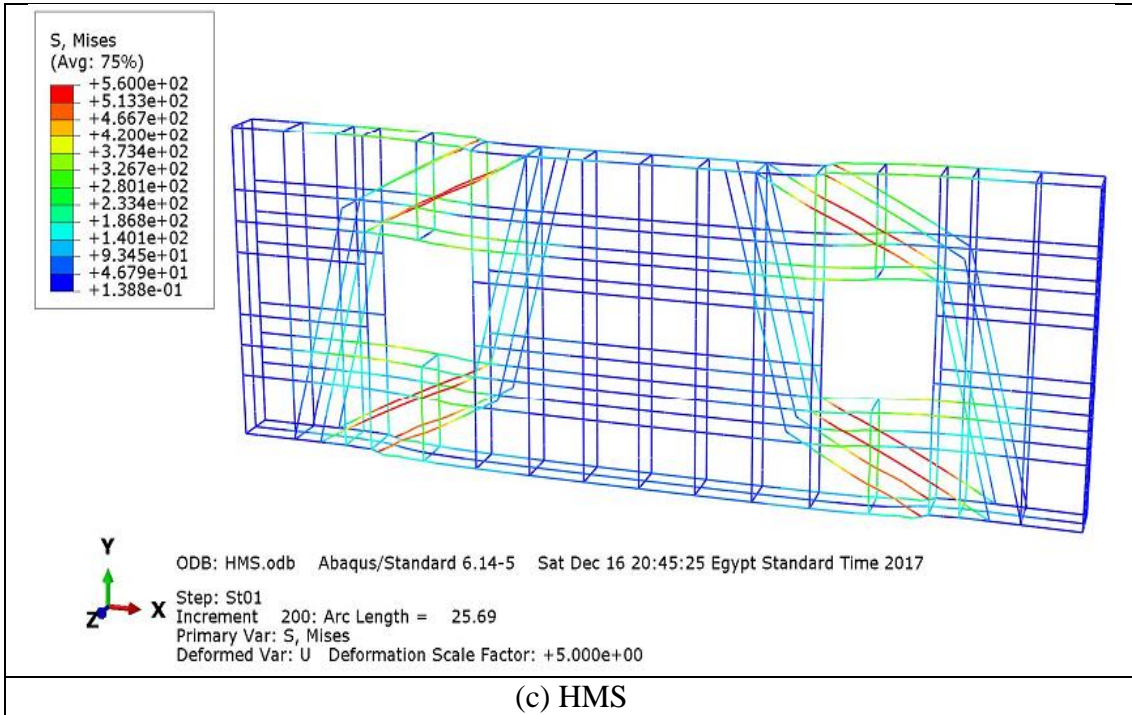
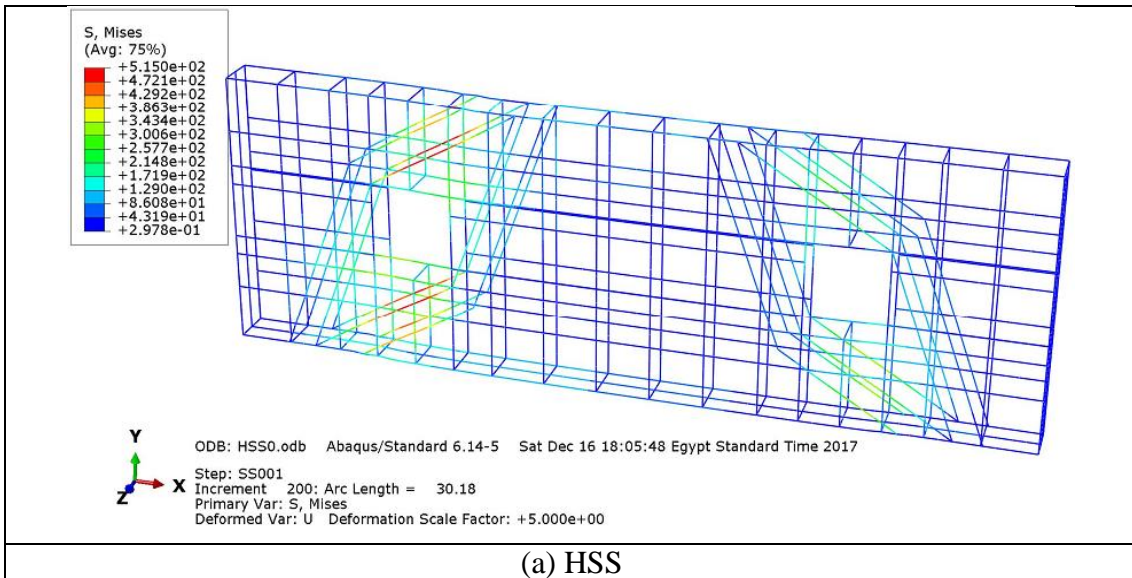


Fig. 26: Stresses in the proposed reinforcement models for beams (a) NLS, (b) HMT, and (C) HMS in the FEM



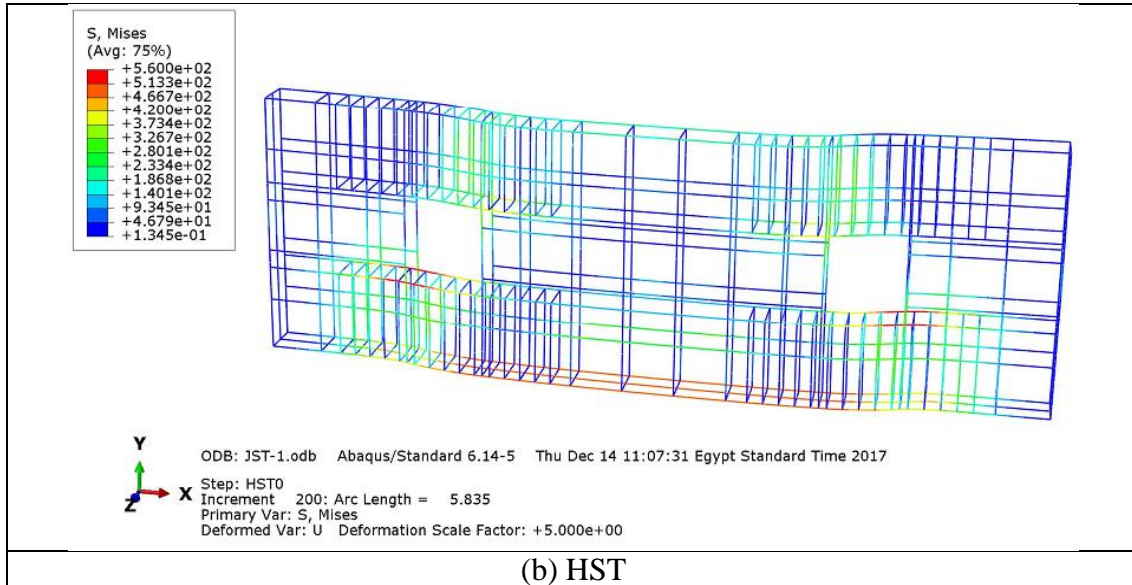


Fig. 27: Stresses in the proposed reinforcement models for beams (a) HSS and (b) HST in the FEM

5. Parametric study

To define the shear strength of the deep beam with shear openings, it first requires knowing the utilized provisions in designing of its similar solid deep beam.

In this parametric study, the ACI 318-14 [1] was used to pre-dimensioning and designing of the solid deep beams and all its requirements were satisfied.

Web reinforcement ratio, main tie reinforcement ratio, L/d ratio, Shear span-to-depth ratio, and strength of both concrete and steel were constant.

Five sizes of deep beams were chosen to represent dimensions of $L \times H \times b$ equal to $1200 \times 600 \times 120$ mm and 4 scales of this size. Scale sizes were 1.5, 2, 3, and 4 respectively

Figure 28 illustrates the general layout of the deep beams with shear openings including used variables in the parametric study.

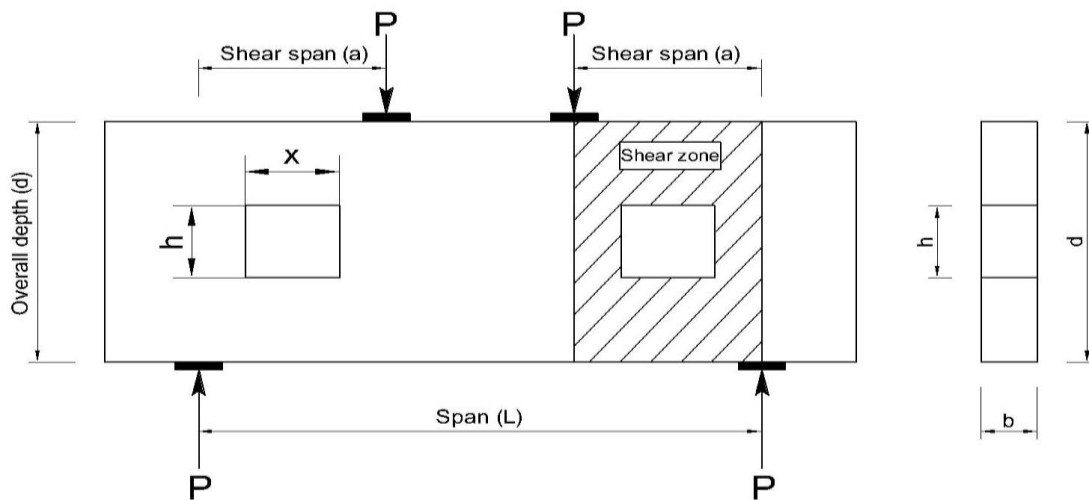


Fig. 28: Dimensions of shear opening and the shear zone in deep beams in the parametric study

Openings in shear zone have three constant ratios of 0.05, 0.094, and 0.15 respectively in comparing to total area of shear zone.

Large, medium, and small shear opening dimensions are $(0.3 \mathbf{d} \times 0.5 \mathbf{X})$, $(0.25 \mathbf{d} \times 0.375 \mathbf{X})$, and $(0.2 \mathbf{d} \times 0.1 \mathbf{X})$ in the vertical and horizontal direction respectively.

Where:

A_o is the area of the shear opening equal to x multiplied by h

x is the horizontal dimension of the shear opening in deep beam.

h is the vertical dimension of the shear opening in the deep beam.

A_{sz} is the total area of the shear zone, equal to a multiplied by d

a defines the shear span which is the horizontal dimension of the overall shear zone in the deep beams (regions from support to concentrated load)

d is the vertical dimension of the shear zone in deep beams, it equal the overall depth of the deep beam.

Table 3 illustrates all specifications and dimensions of the studied deep beams.

Table 3: Properties and dimensions of studied deep beams in parametric study

Scale Factor	No.	Specimen Designation	f'_c (MPa)	Area of opening $x*h$ (mm ²)	Area of shear zone $a*d$ (mm ²)	A_o/A_{sz} ratio	FEM	ACI 318-14	Shear strength relative to solid deep beam
							Load (kN)	Load (kN)	P_o/P_s
Size 1	1	HSD Solid deep beam	50	0	240000	0	544.00	394	
	2	HLR deep beam with large openings		36000	240000	0.15	249.00		0.4577
	3	HMR deep beam with medium openings		22500	240000	0.09375	314.20		0.5776
	4	HSR deep beam with small openings		12000	240000	0.05	390.00		0.7169
Size 1.5	1	HSD	50	0	540000	0	1542.00	1202	
	2	HLR		81000	540000	0.15	971.15		0.6268
	3	HMR		50625	540000	0.09375	1090.20		0.7036
	4	HSR		27000	540000	0.05	1195.20		0.7713
Size 2	1	HSD	50	0	960000	0	1549.50	1669	
	2	HLR		144000	960000	0.15	997.00		0.6434
	3	HMR		90000	960000	0.09375	1081.80		0.6982
	4	HSR		48000	960000	0.05	1225.00		0.7906
Size 3	1	HSD	50	0	2160000	0	5500.00	3686.3	
	2	HLR		324000	2160000	0.15	3901.00		0.7093
	3	HMR		202500	2160000	0.09375	4240.50		0.7710
	4	HSR		108000	2160000	0.05	4496.29		0.8175
Size 4	1	HSD	50	0	2160000	0	6900.00	4949.27	
	2	HLR		576000	3840000	0.15	4816.00		0.6980
	3	HMR		360000	3840000	0.09375	5240.50		0.7595
	4	HSR		192000	3840000	0.05	5498.00		0.7968

*Size 1 represents beam dimensions of 1200x600x120 mm. size 1.5, 2, 3, and 4 represent scale factors of 1.5, 2, 3, and 4 of size 1.

*Shear opening size was limited by $0.3d \times 0.5a$ in the vertical and horizontal directions respectively.

Figure 29 is X-Y plot, which illustrates the relationship between the following:

1. Y-Axis represent the ratio between load capacity of the deep beam with different opening size and the load capacity of the solid deep beam.
2. X-Axis represent the ratio between area of shear opening and the total area of the shear zone.

The lower bound of the relation can be obtained by the following equation, $y = 0.836 - 2.57x$, if we substitute y factor by $\frac{P_o}{P_s}$ and x factor by $\left(\frac{A_o}{A_{SZ}}\right)$ the equation will be in the following form $\frac{P_o}{P_s} = 0.836 - 2.57\left(\frac{A_o}{A_{SZ}}\right)$, which give prediction of the ultimate load of deep beams with shear opening relative to the solid deep beam. Where:

P_s and P_o are the shear strength of the solid deep beam and deep beam with shear openings similar to the solid one, respectively.

P_s will be substituted with the shear strength of the solid deep beam according to ACI 318-14 [1] which is $V_n = 0.83\sqrt{f'_c} bd$

It led to the following dimensionless formula $P_o = 0.83\sqrt{f'_c} bd \left(0.836 - 2.57\left(\frac{x \cdot h}{a \cdot d}\right)\right)$

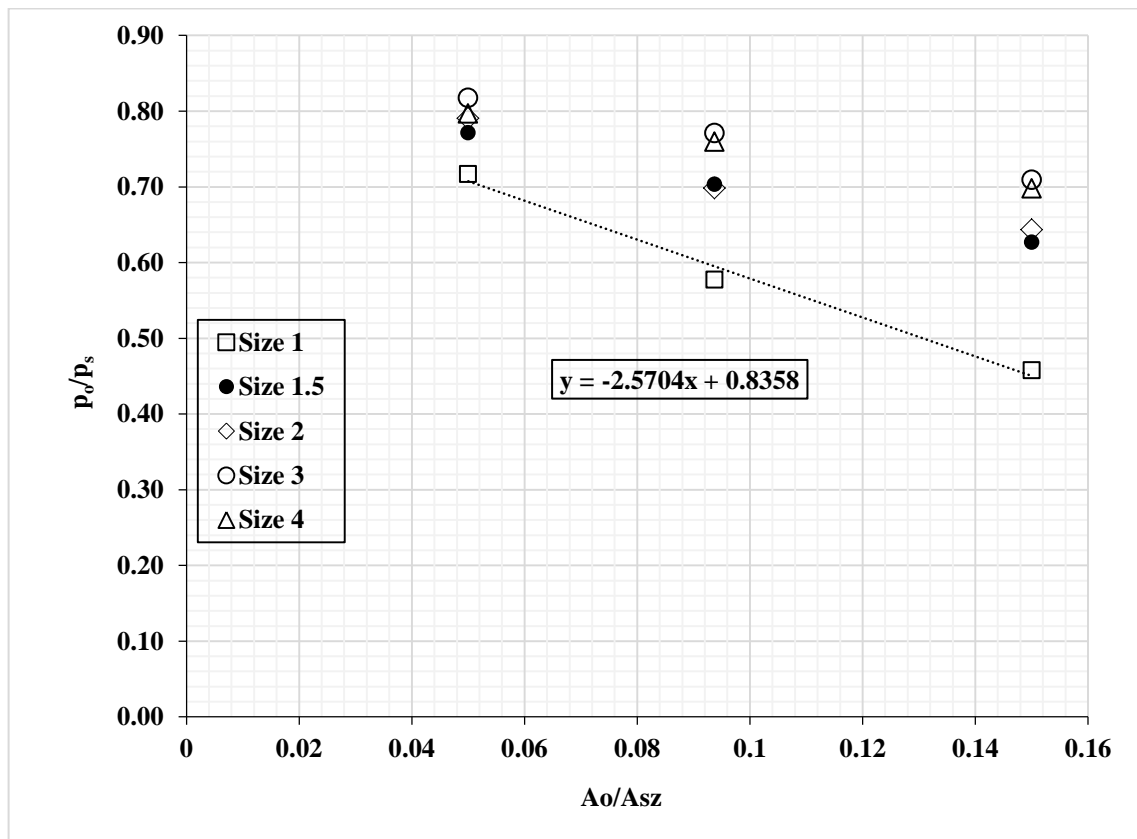


Fig. 29: Relationship between load capacity and the area of opening ratios (5 different sizes)

This proposed equation applies in any deep beams with shear openings which have the same shear span-to-depth ratio (a/d) equal to 0.67.

To verify this equation with other experimental results, Yang et al. [10] tested deep beam with shear span-to-depth ratio of 0.7 which is almost equal studied a/d ratio.

The specifications of the tested deep beam (UH7F3) in Yang et al. [10] and comparison with proposed equation were illustrated in table 4

Table 4: Comparison between proposed equation and other experimental results, Yang et al. [10]

					Experimental	Proposed Equation	Comparison
No	Specimen	f'_c (MPa)	Area of opening x*h (mm)	Area of shear zone a*d (mm)	Load (kN)	Load (kN)	P_{Equ}/P_{Exp}
1	UH7F3	80.4	210x180	420x560	263.60	282	1.07

*a/d ratio equal to 0.7

Table 4 shows the wide range applicability of the proposed equation in case of different concrete strength, opening size, and width of the deep beams.

It worth noted that this deep beams have no transverse web reinforcement, which give indication of the majority of the factor of opening size ratio as in the proposed equation. The previous proposed equations such as Kong and Sharp [11] and Mansur [12] give very conservative prediction of the strength of deep beams with shear openings as certified previously in H. A. Kottb [9] because of underestimate the component of size of opening relative to shear zone.

It also important to point that there is need to derive additional formulas for different a/d ratios to provide full design aid.

6. Conclusions

From this analytical and parametric study it can be concluded that:

- Efficiency of the FE model, in simulating reinforced concrete deep beams with shear openings, was proved by matching with experimental ultimate loads by 97%.
- FE model gives similar crack patterns to the experimental ones and the same trend of the load-displacement response, which verify capability of capturing the real behavior of the deep beams with and without openings.
- The method of embedded strut is more effective in case of angle of inclination not less than 30°.
- The most important component of the two proposed methods is the steel bars adjacent to the shear openings as shown in stresses of steel bars.
- This FE model can be used in predicting the ultimate load of the deep beams with shear openings, while strut-and-tie model of the ACI 318-14 [1] is limited with solid deep beams.
- Stresses in the reinforcement bars at shear zone certify the efficiency of the proposed models.
- Parametric study revealed that as size of deep beam changes from h=600 to 900 mm, significant effect of shear openings on the load capacity is obtained, especially in case of large shear openings.
- The lower bound of the parametric study resulted in an applicable dimensionless formula $P_o = 0.83 \sqrt{f'_c} bd \left(0.836 - 2.57 \left(\frac{x*h}{a*d} \right) \right)$, which recommended in the

design of such beams which have the same shear span-to-depth ratio and the limits of the size of the shear openings.

- The proposed equation give reasonable prediction of the shear strength of deep beams with shear openings in comparing with other experimental result.

References

1. ACI Committee 318. Building Code Requirements for structural concrete (ACI 318-14) and commentary (318R-14). Farmington Hills, MI: American Concrete Institute; 2014. p. 524.
2. ECP 203 Egyptian Code of Practice: Design and construction of reinforced concrete structures, 2007, p. 454.
3. Campione G, Minafò G.: Behavior of concrete deep beams with openings and low shear span-to-depth ratio. *Engineering Structures* 2012; 41(3) 294–306.
4. A. R. Mohamed et al.: Prediction of the behavior of reinforced concrete deep beams with web openings using the finite element method. *Alexandria Engineering Journal* 2014, 53 (2), 329–339
5. W. E. El-Demerdash et al.: Behavior of RC shallow and deep beams with openings via the strut-and-tie model method and nonlinear finite element. *Arab. J. Sci. Eng.* 2016, 41(2), 401-424
6. Abaqus Analysis User's Manual – Abaqus version 6.10 (2016) along year 2017 at <http://abaqusdoc.ucalgary.ca/books/usb/default.htm?startat=pt05ch21s02abm42.html>
7. Nayal R. & Rasheed H. A.: Tension stiffening model for concrete beams reinforced with steel and FRP bars. *Journal of Materials in Civil Engineering* 2006, 19 (6) 831-841
8. E. Hognestad: A study of combined bending and axial load in reinforced concrete members, University of Illinois bulletin 1951, 49 (22)
9. H. A. Kottb "Effect of openings in reinforced concrete deep beams" Ph.D. thesis, Al-Azhar University, Faculty of Engineering, Civil Engineering Department 2017, submitted for revision.
10. Yang et al.: The influence of web openings on the structural behavior of reinforced high-strength concrete deep beams. *Engineering structures* 2006, 28 (13) 1825-1834.
11. Kong F.K., Sharp G. R.: Structural idealization for deep beams with web openings. *Magazine of Concrete Research* 1977, 29 (99) 81–91.
12. Mansur, M. (1998). Effect of openings on the behavior and strength of R/C beams in shear. *Cement & Concrete Composites*, 20 (6) 477–486.